Biometals (2011) 24:645–661
DOI 10.1007/s10534-011-9414-9

Antileukemic activity and cellular effects of rhodium(III) crown thiaether complexes

Ruth Bieda · Igor Kitanovic · Hamed Alborzinia · Andreas Meyer · Ingo Ott · Stefan Wölfl · William S. Sheldrick

Received: 31 October 2010 / Accepted: 12 January 2011 / Published online: 28 January 2011

Abstract The cytostatic properties of novel rhodium(III) thiacrown ether complexes $[RhCl(LL)([9]aneS_3)]^{n+}$ with either aromatic κ^2N ligands ($n = 2$) or anionic chelate ligands ($n = 1$) have been investigated for the human cancer cell lines HT-29 and MCF-7 and for immortalized HEK-293 cells. Taken together with literature IC_{50} values for analogous complexes with polypyridyl ligands or 1,4-dithiane, the in vitro assays indicate that dicationic complexes with soft κ^2N (imino) or κ^2S (thiaether) ligands exhibit significantly higher antiproliferative effects than those with hard κ^2N (amino) ligands. Dicationic complexes are more active than monocationic complexes with similar ligands. Pronounced apoptosis-inducing properties towards Jurkat cells were established for complexes with LL = bpm, dpq, and 1,4-dithiane. The order of activity (bpm > 1,4-dithiane > dpq > bpy) contrasts to that observed for adhesive cancer cells (bpm > bpy, 1,4-dithiane > dpq). Necrosis is insignificant in all cases. The percentage of Jurkat cells exhibiting apoptosis after 24 or 48 h incubation periods is directly correlated to the percentage of cells exhibiting high levels of reactive oxygen species. As established by online monitoring with a sensor chip system, treatment of MCF-7 cells with the bpm and 1,4-dithiane complexes leads to a significant and permanent concentration-dependent decrease in oxygen consumption and cellular adhesion.

Keywords Rhodium · Thiacrown ether · Cytotoxicity · Leukemia · Apoptosis · ROS

Electronic supplementary material The online version of this article (doi:10.1007/s10534-011-9414-9) contains supplementary material, which is available to authorized users.

R. Bieda · W. S. Sheldrick (✉)
Lehrstuhl für Analytische Chemie, Ruhr-Universität Bochum, 44780 Bochum, Germany
e-mail: william.sheldrick@rub.de

I. Kitanovic · H. Alborzinia · S. Wölfl
Institut für Pharmazie und Molekulare Biotechnologie, Ruprecht-Karls-Universität Heidelberg, Im Neuenheimer Feld 364, 69120 Heidelberg, Germany

A. Meyer · I. Ott
Institut für Pharmazeutische Chemie, Technische Universität Braunschweig, Beethovenstraße 55, 38106 Braunschweig, Germany

Introduction

Selective treatment is a prerequisite for all oncological drugs in tumor therapy. As there are currently no tumor therapeutic drugs known without serious side-effects, a high level of current interest is present for research on novel cell selective drugs. Metal compounds can display an advantageous chemical functionality and are currently of increasing interest in medical chemistry, both as diagnostic agents and as drugs (Jakupec et al. 2008; Ott and Gust 2007; Clarke 2002). Only three metal based compounds, cisplatin, carboplatin and oxaliplatin, are currently in use as

antitumor drugs, and all of these contain platinum(II) as the central metal atom. Cisplatin, the most successful metal-containing antitumor therapeutic agent (Rosenberg et al. 1969) is especially active towards testicular and ovarian cancer. Nephro-, oto- and neurotoxicity are unfortunate side-effects, which restrict its clinical utility to a certain extent. Representative examples of non-platinum metal-containing compounds currently in clinical trials are (ImH)[trans-{$RhCl_4$(DMSO)(Im)}] (NAMI-A) and (IndH)[trans-{$RhCl_4(Ind)_2$}] (KP1019) (Jakupec et al. 2008). Whereas the high effectiveness of NAMI-A against metastases is related to a combination of its anti-angionesis and anti-invasive properties against tumor cells and vasculature (Morbidelli et al. 2003), KP1019 entered clinical trials for its activity against colorectal cancer and their metastases (Hartinger et al. 2006; Rademaker-Lakhai et al. 2004). It has been reported, that KP1019 can influence the mitochondrial membrane stability and can activate caspase-3, which is well-known for its induction of apoptosis by the mitochondrial pathway (Kapitza et al. 2005).

Transition metal complexes containing polypyridyl (pp) ligands have recently received considerable attention as potential diagnostic agents owing to their ability to recognize and bind at specific base sequences in DNA (Erkkila et al. 1999; Metcalfe and Thomas 2003). Octahedral Ru(II) and Rh(III) compounds containing the smaller ligands 2,2′-bipyridine (bpy) or 1,10-phenanthroline (phen) have been shown to be groove binders or possible partial intercalators (Erkkila et al. 1999; Zeglis et al. 2007). For larger polypyridyl ligands like phi (9,10-diaminophenanthroline) (Sitlani et al. 1992) and dppz (dipyrido[2,3-*a*:2′,3′-*c*]phenazine) (Frodl et al. 2002) strong intercalative binding has often been established.

$[Rh(phi)_2(phen)]^{3+}$ and $[Rh(phi)(phen)_2]^{3+}$ both display nuclease activity. Whereas $[Rh(phi)_2(phen)]^{3+}$ cleaves in a sequence neutral manner, $[Rh(phi)(phen)_2]^{3+}$ cleaves 5′-pyr-pyr-pur-3′ sequences selectively possibly due to its steric and van der Waals interactions within the major groove [Sitlani et al. 1992). These findings underline the possible influence of the ancillary ligands on both the DNA binding and the biological properties of rhodium polypyridyl complexes. The important role of ancillary ligands in enabling specific DNA site binding is also demonstrated by the H donor ligands en and [12]aneN_4 in $[Rh(en)_2(phi)]^{3+}$ and $[Rh([12]aneN_4)(phi)]^{3+}$, which can recognize 5′-GC-3′ sequences, whereas their structural analogue $[Rh([12]aneS_4)(phi)]^{3+}$ with the H acceptor thiaether coligand [12]ane-S_4 does not (Shields and Barton 1995). Upon irradiation at 311 nm, the phototoxic and photonuclease agent $[RhCl_2(dppz)(phen)]Cl$ exhibits toxicity towards the tumor cell lines GN4, M109 and KB (Menon et al. 2004).

Recent work on the possible anticancer activity of other rhodium(III) polypyridyl complexes has produced some highly promising results. Systematic studies on the cytotostatic properties of the compounds *mer*-$[RhCl_3(DMSO)(pp)]$ and $[(C_5Me_5)RhCl(pp)](CF_3SO_3)$ (pp = bpy, phen, dpq = dipyrido[3,2-*d*:2′,3′-*f*]quinoxaline, dppz, dppn) have demonstrated that the in vitro antiproliferative activities of these contrasting types of rhodium(III) complexes towards the human cancer cell lines HT-29 (colon carcinoma) and MCF-7 (breast carcinoma) increase with increasing polypyridyl ligand size (Harlos et al. 2008; Scharwitz et al. 2008). The meridional trichlorido complexes are extremely potent and exhibit IC_{50} values in the range 0.051–0.095 μM towards the MCF-7 and HT-29 cell lines for the larger polypyridyl ligands pp = dpq, dppz, dppn = benzo[*i*]dipyrido[3,2-*a*:2′,3′-*c*]phenazine (Dobroschke et al. 2009). Significant levels of cell cytotoxicity have also been reported for other rhodium(III) compounds including *mer*-$[RhCl_3(tpy)]$ (tpy = 2,2′:6,2″-terpyridine) (Pruchnik et al. 2002), *fac*-$[RhCl_3([9]aneNS_2)]$ ([9]aneNS_2 = 1-aza-4,7-dithiacyclononane) (Medvetz et al. 2007) and polypyridyl complexes of the types $[RhCl(pp)([9]aneS_3)]^{2+}$ ([9]aneS_3 = 1,4,7-trithiacyclononane) (Bieda et al. 2009a) and $[RhCl(pp)(tpm)]^{2+}$ (tpm = tris(pyrazolyl)methane) (Bieda et al. 2009b) towards adhesive human cancer cell lines. We now report an extension of our previous studies on rhodium(III) crown thiaether compounds to aromatic dinitrogen ligands other than pp (complexes **1**–**4**) (Scheme 1) and to bidentate anionic ligands (complexes **5** and **6**) (Scheme 2). Particular emphasis has been placed on the biological impact of ([9]aneS_3)Rh(III) complexes on non-adhesive leukemia cells.

Results and discussion

Synthesis and structure

An in situ preparation procedure was established for the novel ([9]aneS_3)Rh^{III} complexes of the type

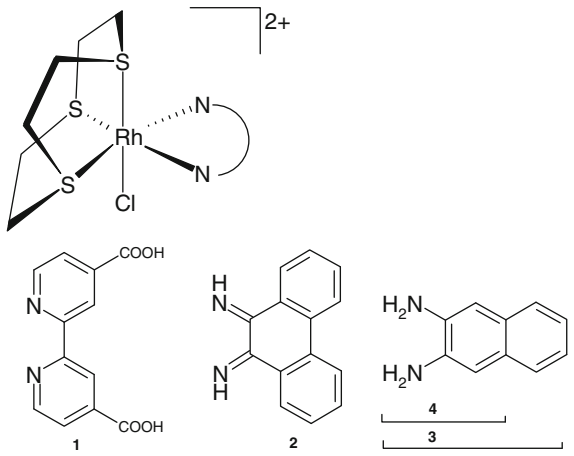

Scheme 1 Structures of the complexes **1**–**4**

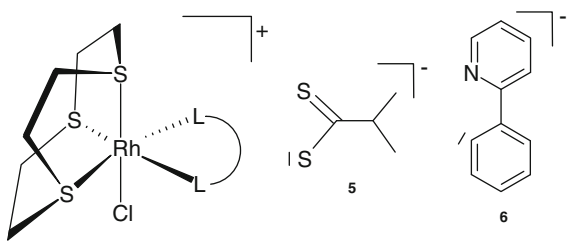

Scheme 2 Structures of the complexes **5** and **6**

$[RhCl(LL)([9]aneS_3)]^{2+}$ **1**–**4** (LL = bpy-4,4′-$(COOH)_2$, phi, naphdiamine, dab,) and $[RhCl(phenylpy)([9]aneS_3)]^{+}$ **6** in accordance to that employed for the previously published compounds $[RhCl(LL)([9]aneS_3)]^{2+}$ **7**–**14** (LL = bpy, bpm = 2,2′-bipyrimidine, phen, tap = pyrazino[2,3-*f*]quinoxaline, dpq, dppz, pip = piperazine, 1,4- dithiane) (Bieda et al. 2009a; 2010). Treatment of $RhCl_3 \cdot 3H_2O$ with the appropriate bidentate (pp) ligand in either CH_3OH, H_2O, CH_2Cl_2 or CH_3OH/CH_2Cl_2 (L) afforded the intermediate complexes $[RhCl_3(pp)(L)]$ in situ which were then employed without further separation or characterization for the preparation of the $[9]aneS_3$ complexes. Compound $[RhCl(dmdtc)([9]aneS_3)]^{+}$ **5** was synthesised by addition of Na(dmdtc) (dmdtc = dimethyldithiocarbamate) to $[RhCl_2(MeCN)([9]aneS_3)]^{+}$ (Bieda et al. 2010) in analogy to the literature procedure for similar complexes with the dithiocarbamate ligands $R_2NCS_2^-$ (R = CH_3CH_2, $PhCH_2$) (Brandt and Sheldrick 1996). Complexes **1**–**6** were characterized by ^1H NMR and positive-ion LSIMS and gave satisfactory microanalyses.

Aromatic diamines of various lengths and shapes were employed as ligands in **2**–**4** to establish whether the activity of these complexes is significantly different from that of compounds containing the larger polypyridyl ligands dpq and dppz. The ligands phi, naphdiamine and dab exhibit the ability to bind to metal atoms either as diimines under abstraction of two protons or as tertiary diamines. In the case of the $([9]aneS_3)Rh^{III}$ compounds **2**–**4,** only 9,10-diaminophenanthrene lost two amino protons during the coordination process to produce the diimino phi complex **2**, as established by LSIMS analysis. The IR spectrum of **2** lacks a strong $\delta(NH_2)$ band in the typical 1,550–1,640 cm^{-1} range for amino complexes and contains only the characteristic weak intensity bands for coordinated phi, namely δ(N–H) at 1,501 cm^{-1} and υ(C=N) at 1,604 cm^{-1}, near to or in this range (Madureira et al. 2000). For the naphdiamine and dab complexes **3** and **4**, LSIMS data clearly indicate a diamino coordination, which is confirmed by the presence of strong $\upsilon(NH_2)$ bands in the range 3,250–3,000 cm^{-1} and strong $\delta(NH_2)$ bands between 1,610 and 1,550 cm^{-1} in both of their IR spectra, e.g. $\upsilon(NH_2)$ at 3,169, 3,134, 3,091 and 3,045 cm^{-1} and $\delta(NH_2)$ at 1,608 and 1,553 cm^{-1} for the naphdiamine complex **3**. The phenomenon of Ru-assisted proton abstraction and diimine coordination has been previously reported for phi and dab compounds (Madureira et al. 2000).

Pronounced antiproliferative activity ($IC_{50} < 12.8$ μM) against MCF-7 and HT-29 cells has previously been established for $([9]aneS_3)Rh^{III}$ complexes containing the κ^2S ligand 1,4-dithiane (Bieda et al. 2010) and the smallest pp ligand 2,2′-bipyridine (Bieda et al. 2009a). We have now employed the anionic κ^2S ligand $dmdtc^-$ in $([RhCl(dmdtc)[9]aneS_3)]^{+}$ **5** and the 2-phenylpyridine ligand $phenylpy^-$ in $[RhCl(phenylpy)([9]aneS_3)]Cl$ **6** to establish whether reducing the overall complex charge to +1 will lead to an increase in activity due to a possible improvement in cellular uptake.

DNA interaction studies

DNA interactions of the $([9]aneS_3)Rh^{III}$ complexes **1**–**6** were investigated together with those of the previously reported complexes $[RhCl(pip)([9]aneS_3)]^{2+}$ **13** and $[RhCl(1,4\text{-dithiane})([9]aneS_3)]^{2+}$ **14** by CD and UV/Vis spectroscopy. Whereas half-sandwich

organometallic complexes with labile chloride ligands typically bind to nucleobase nitrogen atoms (Annen et al. 2000; Sheldrick et al. 1993), those of the type $[(\eta^5\text{-}C_5Me_5)RhCl(pp)]^+$ (pp = dpq, dppz) are strong intercalators into DNA (Herebian and Sheldrick 2002; Scharwitz et al. 2008), and such a binding interaction has also been established for $[RhCl(pp)([9]aneS_3)]^{2+}$ and $[RhCl(pp)(tpm)]^{2+}$ (pp = dpq, dppz) (Bieda et al. 2009a, b). Following initial incubation periods of 5 min, UV/Vis spectra of buffered solutions of complexes **1**–**6** (10 mM phosphate buffer, pH = 7.2) with calf thymus DNA (CT DNA) at 25°C and $r = 0.1$ exhibited no further significant changes over 6 h, thereby indicating that achievement of equilibrium must be rapid. Effectively no absorption changes were observed for complexes $[RhCl(LL)([9]aneS_3)]^{n+}$ **1**–**5**, **13** and **14** on mixing with CT DNA. Only minor changes ($\Delta A/A_{max} = 0.05$ and 0.06) in the DNA absorbance band between 250 and 260 nm were observed for **6** during the initial mixing period.

DNA melting point changes in the presence of a metal compound provide a straightforward method of establishing the strength of DNA binding. The ΔT_m values for CT DNA in the presence of the compounds $[RhCl(LL)([9]aneS_3)]^{n+}$ **1**–**6** were +2, +3, −2, −1, 0 and +1°C, respectively. The negative thermal denaturation temperature changes of −2 and −1°C invoked by the diamino complexes **3** and **4** are in accordance with an absence of intercalation by their aromatic ligands. In contrast, the compounds **1** and **2** with positive ΔT_m values of +2 and +3°C may exhibit groove binding or a limited degree of intercalation. Following the loss of two amino protons during the synthesis of compound **2**, its planar phi ligand can potentially interact with CT DNA in a manner similar to that of the diimino polypyridyl ligands of complexes **9**–**12**. It is interesting to note that ΔT_m values of zero were recorded for the κ^2S coordinated compounds **5** and **14**. Both compounds have, therefore, no significant effect on the stability of the DNA.

In the presence of small molecules, characteristic changes in the circular dicroism (CD) spectra of DNA in the range of 220–400 nm can provide a means of monitoring possible conformational changes for the biopolymer (Brabec et al. 1990; Eriksson and Norden 2001). CT DNA is present in the B DNA form for which a negative CD band at 246 nm caused by the helical conformation and a positive CD band at 275 nm due to base stacking are observed. Changes induced by specific interactions between the biomolecule and the aromatic ligand of the transition metal complexes can induce CD bands between 280 and 400 nm as a result of intercalation, surface or groove binding. Only very minor changes in the DNA conformation were established on addition of the compounds **1**, **2** or **6**. Small differences are apparent in Fig. S1 for the induced CD signal related to the base stacking of CT DNA in the presence of **5** or **14** {r = [complex]/[DNA] = 0.2 for [DNA] = M (bp)} in a 10 mM phosphate buffer. The molar ellipticity [θ] decreased by 10% for **5** but increased by 5% for **14** at the maximum of the positive CD band at 275 nm.

Small decreases in the ellipticity value for the base stacking signal were also observed for CT DNA in its mixtures with **2** or **4** (Fig. 1). In striking contrast, the CD spectrum of compound **13** with CT DNA at $r = 0.2$ displayed a pronounced decrease of 52% in the magnitude of the band related to base stacking. Whereas the helix conformation is apparently little affected by this interaction, the base stacking signal is reduced to nearly half its original value. This change could result from covalent binding of the rhodium fragment to the double helix, for which additional evidence is provided by the observed ΔT_m value of −2°C. Although this compound causes significant changes in the DNA conformation, it does not exhibit significant cytostatic activity ($IC_{50} > 100$ μM) towards the adenomacarcinoma MCF-7 and HT-29 cells. In contrast, whereas the diimino phi complex **2** causes only minor changes for both the characteristic DNA CD signals, it invokes relatively low IC_{50} values of 19.20 (2.19) μM and 11.96 (1.93) μM in MCF-7 and HT-29.

Cellular effects

Antiproliferative activity towards adhesive MCF-7, HT-29 and HEK-293 cells

In vitro studies on the antiproliferative activities of compounds of the type $[RhCl(LL)([9]aneS_3)]^{n+}$ **1**–**6** were carried out with the human MCF-7 (breast cancer) and HT-29 (colon cancer) cell lines and the resulting IC_{50} values are listed in Table 1 together with those for the ligands LL in Table 2. Estimated

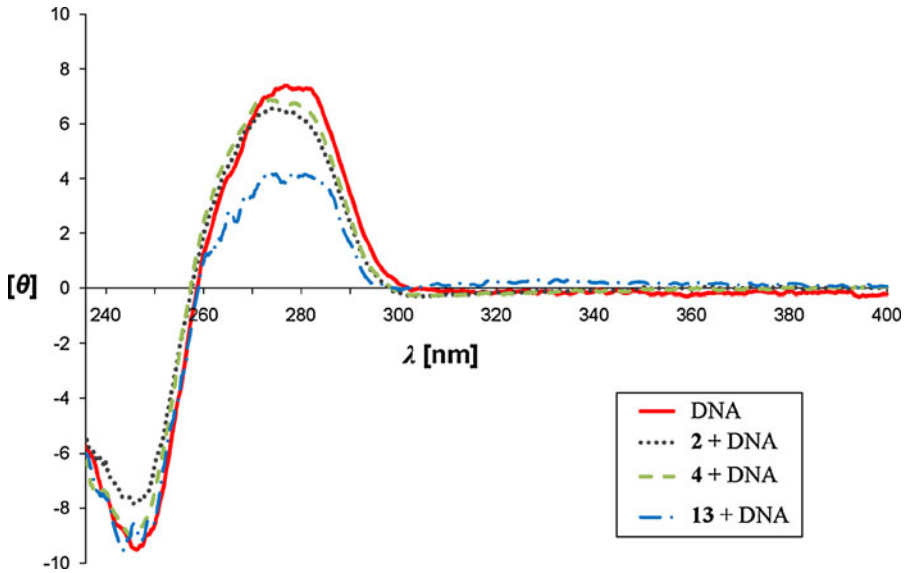

Fig. 1 CD spectra of CT DNA and mixtures of $[RhCl(phi)([9]aneS_3)]Cl_2$ **2**, $[RhCl(dab)([9]aneS_3)]Cl_2$ **4** and $[RhCl(pip)([9]aneS_3)]Cl_2$ **13** with CT DNA {r = [complex]/[DNA] = 0.2 for [DNA] = M (bp)} in a 10 mM phosphate buffer (pH = 7.2) after an incubation period of 1 h. Molar ellipticities [θ] are given in the units deg cm^2 $dmol^{-1}$ × 10^{-3}

Table 1 IC_{50} (μM) values for the complexes $[RhCl(LL)([9]aneS_3)]^{n+}$ **1–14**

Compound	LL	Counter ions	MCF-7 IC_{50}	HT-29 IC_{50}	HEK-293 IC_{50}
1	bpy-4,4′$(COOH)_2$	Cl_2	>100	>100	>100
2	Phi	Cl_2	19.20 (2.19)	11.96 (1.93)	26.1 (5.0)
3	Naphdiamine	Cl_2	18.06 (3.42)	50.7 (5.8)	>100
4	Dab	Cl_2	>100	>100	>100
5	Dmdtc	CF_3SO_3	33.1 (2.1)	40(27)	94.1 (0.5)
6	Phenylpy	Cl	57.3 (9.0)	51.6 (17.3)	54.1 (7.2)
7[a]	Bpy	Cl_2	12.8 (0.2)	4.4 (0.1)	>100
8[a]	Bpm	Cl_2	1.7 (0.5)	1.9 (0.1)	0.6 (0.2)
9[a]	Phen	$[PF_6]_2$	36.3 (6.0)	72.2 (8.0)	>100
10[a]	Tap	Cl_2	11.5 (0.6)	7.6 (4.8)	3.3 (1.3)
11[a]	Dpq	Cl_2	19.1 (0.3)	20.9 (2.8)	45.5 (1.9)
12[a]	Dppz	Cl_2	4.7 (0.5)	7.4 (2.2)	8.9 (1.6)
13[b]	Pip	Cl_2	>100	>100	>100
14[b]	Dithiane	Cl_2	9.6 (2.2)	8.1 (3.7)	11.6 (2.9)

Estimated standard deviations are given in parentheses

[a] Bieda et al. (2009a)

[b] Bieda et al. (2010)

standard deviations are given in parentheses. To determine a possible cell selectivity of facial Rh(III) compounds towards cancer cell lines, these compounds were also tested towards immortalized HEK-293 (human embryonic kidney) cells (Table 1).

The expected trend of increasing antiproliferative activity with increasing length of the polypyridyl ligand (Schäfer et al. 2007) has been established for the analogous tpm compounds (Bieda et al. 2009b) against the cancer cell lines MCF-7 and HT-29 and in

Table 2 IC_{50} (μM) values for selected ligands

Ligand	MCF-7 IC_{50}	HT-29 IC_{50}	HEK-293 IC_{50}
$bpy(COOH)_2$	>100	>100	ND
phi	19.5 (1.5)	15.6 (3.0)	29.2 (9.6)
naphdiamine	43.9(29.0)	63.5(4.5)	>100
dab	37.0(12.6)	58.8(16.6)	65.6 (4.0)
phenylpy	>100	>100	>100
Cisplatin[a]	2.0 (0.3)	7.0 (2.0)	2.6 (0.6)

Estimated standard deviations are given in parentheses

[a] Scharwitz et al. (2008)

the case of the [9]aneS_3 compounds for **9**, **11** and **12** containing the larger polypyridyl ligands phen, dpq and dppz (Bieda et al. 2009a). This trend is also followed by the IC_{50} values for the ([9]aneS_3)Rh^{III} compounds towards HEK-293 cells. A different mechanism of action was postulated for compounds containing the nitrogen-rich bpm and tap ligands on the basis of their high antiproliferative activity (Bieda et al. 2010). The results presented in Table 1 allow two structure–activity relationships to be established. Firstly, complexes containing diamino ligands are, in general, less active than κ^2N (imino) coordinated complexes. Secondly, as exemplified by complex **6** in comparison to its κ^2N (imino) analogue **7**, overall charge reduction from +2 to +1 appears to lead to a loss of activity. It is interesting to note, in this respect, that following deprotonation of its carboxylate functions, the inactive complex **1** will exhibit overall neutrality at biologically relevant pH values. However a reduced level of cellular uptake could also be responsible for its lack of antiproliferative activity.

IC_{50} values >100 μM towards all three cell lines were established for the diamino complexes **4** and **13**. In comparison, the diimino phi complex **2** exhibits values of 19.20 (2.19) (MCF-7), 11.96 (1.93) (HT-29) and 26.1 (5.0) μM (HEK-293), that are comparable to those of the dpq complex **11**. When compared to the likewise very similar values of 19.5 (1.5) and 15.6 (3.0) μM for the ligand itself towards MCF-7 and HT-29 cells, it can be postulated that the activity of **2** may primarily be due to the spatial and stacking properties of the phi ligand on its own. Whereas the dab compound **4** exhibits no significant antiproliferative activity towards either MCF-7 or HT-29 cells ($IC_{50} > 100$), IC_{50} values of 18.06 (3.42) μM and 50.7 (5.8) μM towards the cancer cell lines were established for complex **3** with its larger aromatic surface area. As no activity was observed towards HEK-293 cells, it is apparent that the cell lines exhibit increasing sensitivity towards this complex in the order MCF-7 > HT-29 ≫ HEK-293, which may be related to the cytotostatic properties of the diamino ligand on its own. For naphdiamine itself, IC_{50} values of 43.9(29.0) and 63.5(4.5) μM were observed towards MCF-7 and HT-29 cells, respectively, but the IC_{50} value was greater than 100 μM for HEK-293 cells.

Apoptosis induction in the leukemia cell lines K562 and Jurkat

We extended the biological studies on ([9]aneS_3)Rh^{III} complexes to the non-adhesive leukaemia cell lines K562 and Jurkat. The compounds **7**, **8**, **10**, **11** and **14** were selected on the basis of their relatively high antiproliferative activities (Table 1) towards the adhesive cell lines MCF7 and HT-29 and their differing types of bidentate ligands. Apoptosis induction was tested for K562 (human chronic myelogenous leukemia) and Jurkat cells (human T-cell leukemia) by an Annexin V/propidium iodide assay and PARP cleavage. The biological impact of the compounds was followed by measuring the intracellular level of reactive oxygen species (ROS) and by online monitoring of cellular metabolic processes.

In apoptotic cells, phosphatidylserine is translocated from the inner to the outer leaflet of the plasma membrane, thereby exposing it to the external cellular environment (van Engeland et al. 1998), where it can be detected by its binding to the intracellular protein Annexin V (Andree et al. 1990), labeled with a fluorophore (Koopman et al. 1994). An Annexin V assay is able to distinguish apoptotic cells from viable or necrotic cells on the basis of the resulting fluorescence of the former cells. A simultaneous dead cell stain employs the fluorochrome propidium iodide (PI), that can only penetrate dead or dying cells that have lost or are losing membrane integrity. PI intercalates into DNA to produce a highly fluorescent adduct, that enables a precise evaluation of cellular DNA content by flow cytometric analysis (Lecoeur 2002; Riccardi and Nicoletti 2006). PI positivity is an indicator of either late apoptosis or necrosis.

Annexin V/PI assays were first performed for K562 cells with complexes **7**, **10** and **11**. After 48 h

incubation periods with concentrations of 10, 20 and 40 μM, the cells were, however, only affected in a minor fashion (data not shown). The percentage of viable cells was higher than 80% in all cases. Mock (solvent of the highest concentration) and 5 μM CMPT (camptothecin) samples were employed as controls. Assays were then carried out for Jurkat cells after 24 and 48 h incubation periods with the same complexes. No significant apoptosis was determined after 24 h, which indicates that reduced cell viability is a time-dependent process (data not shown). Figure 2 depicts the state of the Jurkat cells for each of the three compounds in correlation to the number of cells/ml present after the 48 h incubation periods. All three compounds reduced the total cell number in a concentration-dependent manner. In comparison to the control value of nearly 6×10^5 cells/ml, compound **7** containing the smaller bpy ligand lowered the numbers of cells only gradually in dependence on its concentration to a final cell number of nearly 4×10^5 cells/ml for a 40 μM solution. After treatment with a 10 μM solution of the tap complex **10**, the viable cell number was lowered to about 5.3×10^5 cells/ml and this value was further reduced to about 3.5×10^5 cells/ml at a concentration of 40 μM. The most pronounced cell number decrease was determined in the case of complex **11** with the largest polypyridyl ligand. After treatment with a 10 μM concentration of the dpq complex about 2.9×10^5 cells/ml were still viable. Only 2×10^5 cells/ml were viable in the case of a 20 μM solution and this number fell to 1.4×10^5 cells/ml for the 40 μM solution. The extent of apoptosis induction was not as high as observed for the CMPT control, but the reduction in the number of cells/ml to about only a quarter of the control value is indicative of pronounced anti-proliferative properties of the dpq-containing ([9]aneS$_3$)Rh^{III} complex towards Jurkat cells. It is interesting to note that complex **11** has a markedly lower antiproliferative effect towards the adhesive cell lines MCF-7 and HT-29 than complexes **7** and **10** (Table 1). The findings of Fig. 2 therefore indicate an increased sensitivity of Jurkat cells towards **11** in comparison to **7** and **10**.

Effectively no cell death inducing properties were established for compound **7** towards the Jurkat cells. The percentage of viable cells decreased only marginally from 96 to 93% with increasing concentration (10–40 μM) of **7**. Decreasing percentages of viable

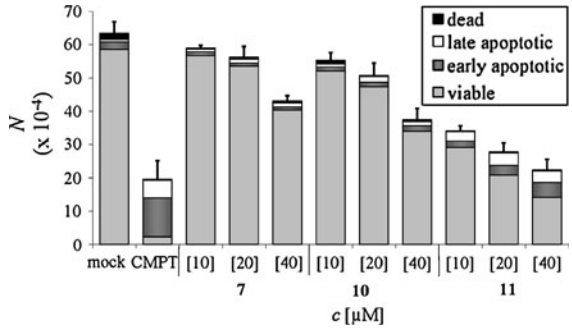

Fig. 2 Annexin V/PI assay towards Jurkat cells illustrating the number of cells/ml following their 48 h treatment with the compounds **7**, **10** and **11** at various concentrations. *N* gives the number of cells/ml. Mock (solvent of the highest concentration) and 5 μM camptothercin (CMPT) samples were employed as controls

cells correlating to increasing relative amounts of early and late apoptotic cells were more apparent for compound **10** and particularly for **11** after the longer incubation period. Compound **11** induces apoptosis in a clearly concentration-dependent manner. After a 48 h incubation with a 10 μM solution of **11**, 87% viable Jurkat cells were established, for a 20 μM concentration 74% and for a 40 μM concentration only 63%. In conclusion, the data of the Annexin V/PI assay for the compounds **7**, **10** and **11** towards the Jurkat cells demonstrate that with increasing size of the polypyridyl ligand (bpy < tap < dpq) increasing apoptosis induction is invoked within a 48 h incubation period, whereas after 24 h no significant apoptosis induction could be established. This order of activity contrasts to that observed for the adhesive MCF-7 and HT-29 cells (dpq < bpy < tap) and suggests that cell-type differences in the mechanism of action may play a role.

These findings prompted us to study the impact of two further rhodium(III) complexes **8** and **14** on Jurkat leukemia cells. The former bpm complex exhibits the lowest IC_{50} values of all previously tested ([9]aneS$_3$)Rh(III) complexes (Table 1) and the latter compound contains an aliphatic κ^2S chelate ligand rather than the aromatic κ^2N (imino) ligands of **7**, **8**, **10** and **11**.

In the case of complex **8** a high antiproliferative activity was also established for the non-adhesive Jurkat cells (Fig. 3). No necrotic cells were observed. Even at the lowest concentration of 1.25 μM, the cell number was reduced after 48 h to about a half in

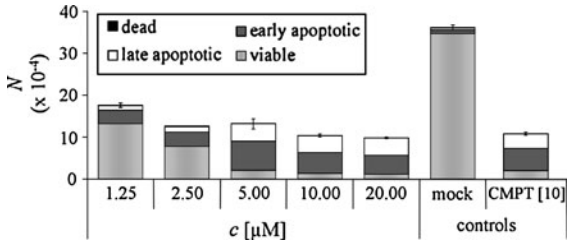

Fig. 3 Annexin V/PI assay towards Jurkat cells illustrating the number of cells/ml following their 48 h treatment with the compound $[RhCl(bpm)([9]aneS_3)]^{2+}$ **8** at various concentrations. *N* gives the number of cells/ml

comparison to the mock control sample. At 20 μM only 1.0×10^5 cells/ml were present in comparison to 3.6×10^5 cells/ml for the control. Following treatment with a 5 μM solution nearly all cells were in an early or late apoptotic state. On increasing the concentration up to 10 and 20 μM, the percentages of cells undergoing early or late apoptosis were comparable to those found for cells treated with CMPT at 10 μM.

Figure 4 illustrates the numbers of Jurkat cells/ml following treatment with the 1,4-dithiane complex **14** at various concentrations for 48 h. Though lower than for the bpm complex **8**, a much stronger antiproliferative effect was apparent in comparison to the polypyridyl complexes **7** and **11**. While the percentage of viable cells was similar to the percentage of late and early apoptotic cells for a 10 μM solution, no vital cells could be detected at a 20 μM concentration. Although its antiproliferative properties are less pronounced at lower concentrations (<5 μM), the dithiane complex **14** exhibits similar apoptosis-inducing properties to the bpm complex **8** at higher concentrations. As for the dpq complex **11**, the Jurkat cells appear to be significantly more sensitive towards **14** than are the adhesive MCF-7 or HT-29 cells.

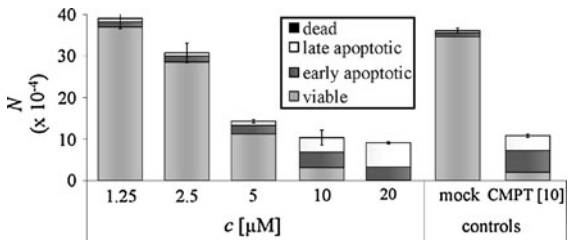

Fig. 4 Annexin V/PI assay towards Jurkat cells illustrating the number of cells/ml following their 48 h treatment with the compound $[RhCl(dithiane)([9]aneS_3)]^{2+}$ **14** at various concentrations

PARP cleavage assay

For confirmation of caspase activity and apoptosis induction, Western Blot analyses were performed for possible PARP cleavage products. The DNA repair enzyme PARP [poly (ADP-Ribose) polymerase] is expressed more in apoptotic cells due to DNA fragmentation and is cleaved by caspases, especially by caspase-3 in vivo (Nicholson et al. 1995). The inhibition and cleavage of PARP protein can therefore be considered as being molecular markers for caspase-mediated apoptosis. An antibody against PARP can detect intact PARP (116 kDa) and its cleavage products (89 and 24 kDa). Western Blot analysis for anti-β-actin obtained from the same membrane was used as a loading control to verify the total protein content. The Western Blot analyses of possible cleavage products of the PARP protein in Jurkat cells after a 24 h treatment at the indicated concentrations of the substances **11** and **7** are depicted in Fig. 5. This pair was chosen to enable a comparison of possible caspase activity for complexes with markedly different activities towards the leukemia cells.

A 10 μM solution of complex **11** induced a significant degree of apoptosis in Jurkat cells and activation of mitrochondia-dependent caspase cascades led to PARP cleavage to the 89 kDa product by caspase-3. The 89 kDa fragment was much less intensive for a 20 μM solution and could not be clearly visualized at a concentration of 40 μM despite comparable loading. As this fragment just represents an initial step in PARP cleavage and degradation and the process of caspase-mediated apoptosis is accelerated and/or enhanced at higher concentrations, it can be assumed that further PARP degradation must

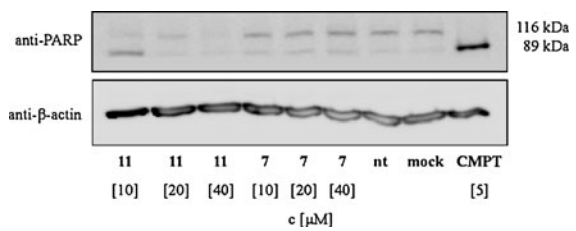

Fig. 5 Western Blot (WB) analyses of Jurkat cells after 24 h treatment. **a** anti-PARP (*top*) with 116 kDa PARP and 89 kDa cleaved PARP and **b** Western Blot: anti-β-actin (42 kDa) used as a detector for the applied amount of protein in each case. *NT* not treated

have taken place for the 20 and 40 μM solutions of **11**. For the effectively inactive compound **7** (see Fig. 2), no significant PARP cleavage product of 89 kDa could be determined even at the higher concentrations of 20 and 40 μM. 5 μM Camptothecin was used as a positive probe for caspase-induced apoptosis and PARP cleavage.

Measurements of reactive oxygen species (ROS)

An increase of intracellular reactive oxygen species (ROS) is correlated to a deregulated mitochondrial activity, which is an additional indication of apoptosis induction and may reflect overall stress. The occurrence of ROS was measured for Jurkat cells by flow cytometry analysis and is shown in Figs. 6, 7 and 8 as high and low ROS levels. After given incubation periods, the detection marker dihydroethidium bromide (DHE) was applied and the levels of high and low ROS were measured by FACS (fluorescence-activated cell sorting). The effects of the less active complex **7**, and the three compounds **8**, **11** and **14** with pronounced antileukemic activity were determined for Jurkat cells after 24 and 48 h treatments.

Significantly enhanced levels of intracellular ROS were observed after 24 h treatments with each of the

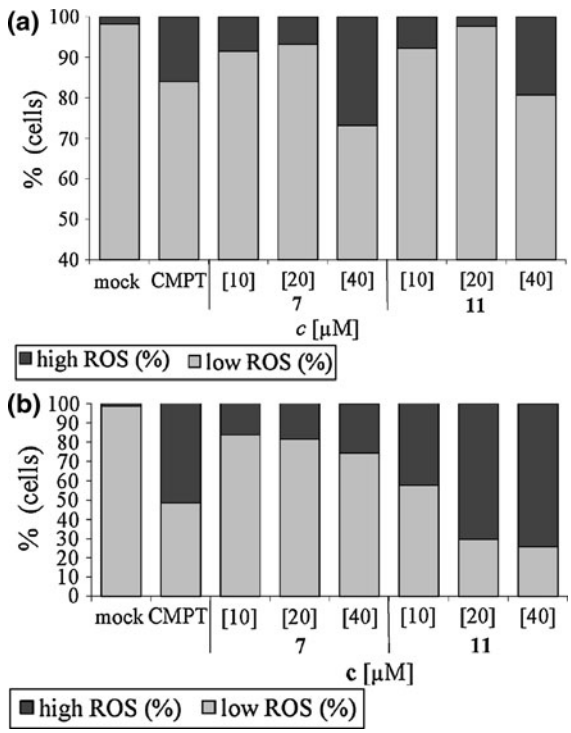

Fig. 6 Percentages of cells exhibiting high ROS levels in Jurkat cells in the presence of $[RhCl(bpy)([9]aneS_3)]^{2+}$ **7** and $[RhCl(dpq)([9]aneS3)]^{2+}$ **11** after incubation times of **a** 24 h and **b** 48 h

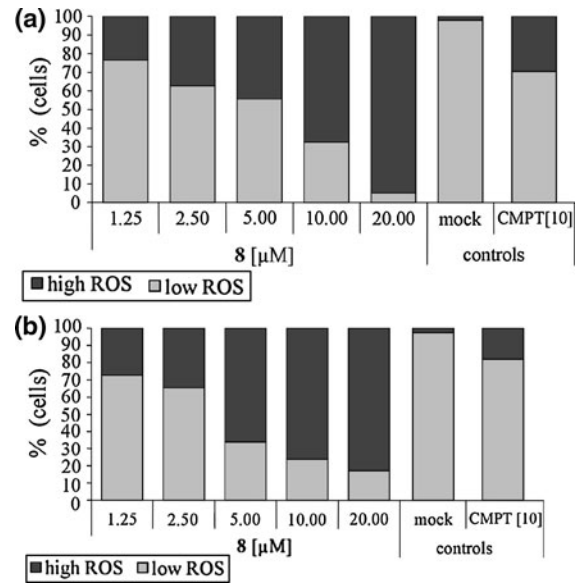

Fig. 7 Generation of reactive oxygen species in Jurkat cells in the presence of $[RhCl(bpm)([9]aneS_3)]^{2+}$ **8** after incubation times of **a** 24 h and **b** 48 h

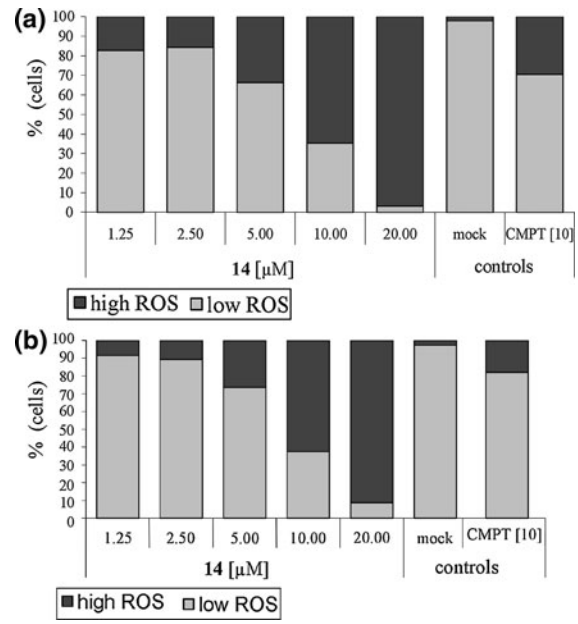

Fig. 8 Percentages of cells exhibiting high ROS levels in Jurkat cells in the presence of $[RhCl(1,4\text{-dithiane})([9]aneS_3)]^{2+}$ **14** after an incubation time of **a** 24 h and **b** 48 h

complexes at a 40 μM concentration. After a 48 h incubation, the percentages of cells exhibiting high ROS levels differed more strikingly than for the shorter time period (Fig. 6). Intracellular ROS were generated at significantly higher levels at all concentrations of **11**. For compound **7**, the increases in the percentages cells exhibiting high ROS (17–26%) now correlated with increasing concentration. However ROS levels did not significantly differ from those recorded after only 24 h. **11** is clearly more active than **7** after 48 h. 20 and 40 μM solutions of **11** induced high ROS levels for 70 and 74% of the cells (Fig. 6b), whereas CMPT only induced high ROS levels in 52% of cells at a concentration of 20 μM.

It is instructive to compare Fig. 6 with the results obtained for the potent bpm compound **8** after 24 and 48 h (Fig. 7). This also invoked increasing percentages of cells with high ROS levels with increasing compound concentration. Whereas at a 1.25 μM concentration, 27% of the Jurkat cells already exhibited high ROS levels, this number rose to 83% for a 20 μM solution of **8** following a 48 h incubation period (Fig. 7b). However, in striking contrast to the less active dpq complex, the percentages of cells exhibiting high ROS levels were already very high after 24 h and comparable to those observed for the longer incubation period.

Figure 8 displays the concentration-dependent percentages of Jurkat cells with high ROS levels after 24 and 48 h treatments with **14**. Incubation of the leukemia cells with a 10 μM solution of **14** induced threefold more cells with high ROS than CMPT and at a concentration of 20 μM of **14** more than 90% of the cells exhibited high ROS levels. As also established for the potent complex **8**, no effective increase in the percentages of cells exhibiting high ROS levels was observed in the time period 24–48 h.

In summary, a clear correlation between the percentage of cells exhibiting high ROS levels and the percentage of apoptotic cells was apparent after 48 h treatments with the potent complexes **8**, **11** and **14**. This finding is in accordance with studies that have indicated that higher levels of reactive oxygen species have a destructive effect on DNA and some proteins and that the associated oxidative stress can trigger apoptosis (Simon et al. 2000; Sandstrom et al. 1994). It is particularly interesting, that the aliphatic 1,4-dithiane complex **14** induced high ROS concentrations similar to those of complex **8**, although it does not contain an aromatic diimino donor ligand, whose abilitiy to invoke ROS through either irradiation or through reactions with cellular reductants is well-documented (Levina et al. 2009; Wang et al. 2010).

Cellular metabolism

A cell-based sensor chip system was employed to monitor the influence of complexes **8** and **14** on the metabolism of MCF-7 cells. This system allows the online evaluation of the impedance of the cell layer, oxygen consumption and the extracellular acidification rate (glycolysis) of living cells over an extended time span. Its silicon chip includes interdigitated electrode structures for measuring the cellular impedance (Ehret et al. 1998), miniature Clarke-type oxygen electrodes for monitoring the cellular oxygen uptake (Wolf et al. 1998) and ion-sensitive field effect transistors to record extracellular pH changes (Lehmann et al. 2000).

The impedance of the MCF-7 cell layers fell rapidly almost immediately after treatment begin with 50 μM solutions of **8** and **14** and reached a steady percentage level of about 25% of its initial value after 20 h in both cases (Fig. 9). This decrease indicated either morphological changes and/or changes in the status of cellular adhesion properties, including cell–cell and cell–matrix contacts, corresponding to the

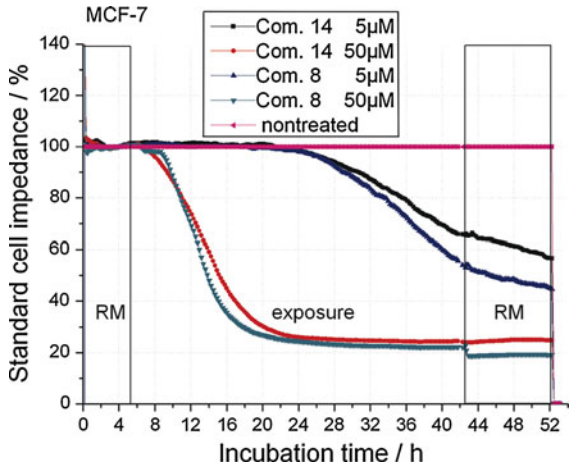

Fig. 9 Standard cell impedance (%) for MCF-7 cells over a 38 h exposure period with 5 and 50 μM solutions of compounds **5** and **8**. The end of treatment is indicated by a *vertical line*. Measurements were continued for an additional 9 h after removal of the substances. *RM* running medium

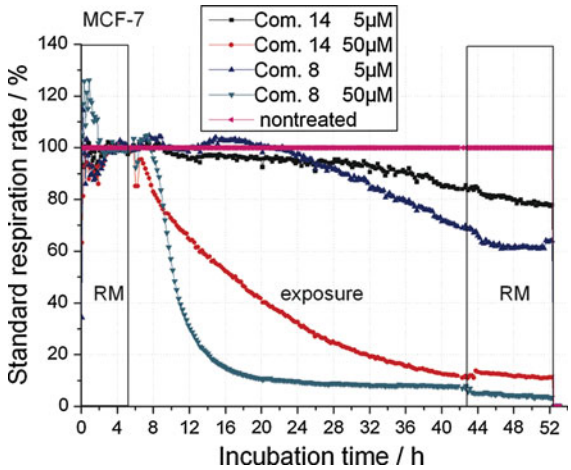

Fig. 10 Standard respiration rates (%) for MCF-7 cells over a 38 h exposure period with 5 and 50 μM solutions of compounds **5** and **8**. The end of treatment is indicated by a vertical line. Measurements were continued for an additional 9 h after removal of the substances. *RM* running medium

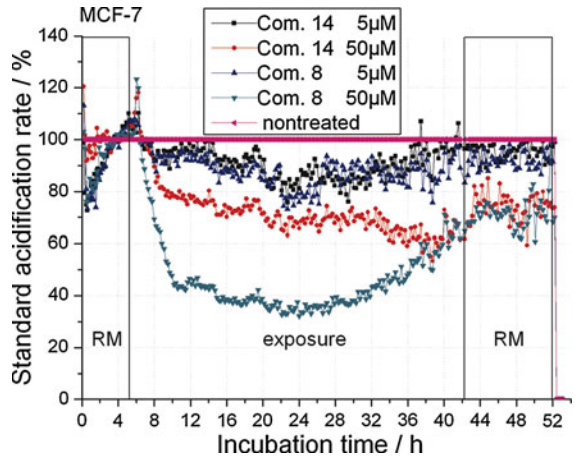

Fig. 11 Standard extracellular acidification rates (%) for MCF-7 cells over a 38 h exposure period with 5 and 50 μM solutions of compounds **5** and **8**. The end of treatment is indicated by a *vertical line*. Measurements were continued for an additional 9 h after removal of the substances. *RM* running medium

induction of cell death. The impact of 5 μM solutions first became apparent after 16 h. A less rapid decline in the impedance of the cellular layer was then observed but this continued during the final drug free period (43–52 h), which indicated the infliction of permanent cellular damage at concentration levels close to the IC_{50} values of **8** and **14** (Figs. 3, 4).

Oxygen consumption is generally indicative of enhanced or decreased mitochondrial activity (respiration). Other oxygen consuming processes are much less efficient and thus unlikely to contribute significantly to this signal. From Fig. 10, it is apparent that the oxygen consumption of the MCF-7 cells was dramatically affected during the first hours of treatment with 50 μM solutions of **8** and **14** and fell to a relative level of about only 10–15% after 16 and 38 h, respectively. No recovery was observed in the final drug free phase. Significant decreases in the respiration rates for the MCF-7 cells first became apparent during the second day of treatment (28–43 h) with the 5 μM solutions. The relative values only fell to about 70 and 80% for cells treated with **8** and **14**, respectively, but no recovery was observed during the drug free period. This permanent reduction in cell respiration correlates well with the likewise dose-dependent increase in intracellular ROS levels in Jurkat cells following their treatment with the complexes (Figs. 7, 8).

Extracellular acidification is closely linked to the activity of glycolysis. This parameter is chiefly influenced by lactic acid production, which is a waste product of anaerobic metabolism. 50 μM solutions of **8** and **14** both invoked significant decreases in the extracellular acidification rate for MCF-7 cells within the first hours of treatment (Fig. 11), which indicates a lower cellular activity in comparison to nontreated cells. After reaching minimum values of about 80–88% following treatment for 20–30 h, the acidification rates increased slowly for cells treated with 5 μM solutions of the complexes during the final hours of treatment. Interestingly, an increase was also observed for the cells treated with the 50 μM solution of **8** during this period, although their acidification rate had fallen to about only 35% of the original value after a 20 h exposure. All in all, the 38 h treatments had only a minor long-term effect on the extracellular acidification rate even at the higher concentration.

Conclusions

The complexes $[RhCl(LL)([9]aneS_3)]^{2+}$ with LL = bpm (**8**) and 1,4-dithiane (**14**) are potent antiproliferative agents towards both adherent cancer cells and non-adherent leukemia cells. In contrast, a total lack of activity was established for the complexes **4** and

13 with the diamino chelate ligands 1,2-diaminobenzene (dab) and piperazine (pip), which suggests that the presence of bidentate ligands with soft donor atoms may well be a prerequisite for high activity in this type of complex. Reducing the overall charge from +2 to +1 also led to a significant loss of activity for the complexes **5** and **6**.

Complexes **8** and **14** induce apoptosis in Jurkat cells but cause negligible necrosis. A high percentage of Jurkat cells exhibit high ROS levels after 24 h treatments with these complexes at concentrations in the 5–20 μM range and these percentages remain effectively constant over the next 24 h. Annexin V/PI assays indicate that the apoptosis levels are directly correlated to the cellular ROS concentrations after 48 h, which suggests that the associated oxidative stress must play a central role in the mechanism of action of the thiaether complexes. Cellular metabolism studies demonstrated that the apoptosis induction is time-dependent at concentrations close to the compounds' IC_{50} values. Cell death induction was first apparent after about 16 h but then increased steadily over the following 24 h and during the drug free period. A similar time-dependent permanent decrease was also established for the cellular respiration rate.

Our present findings for complex **14** demonstrate that the presence of an aromatic diimino chelate ligand is not essential for high antiproliferative activity but rather the presence of five soft donor atoms (i.e., 5 thiaether S atoms or 3 thiaether S atoms plus 2 imino N atoms) in the octahedral coordination sphere of the rhodium(III) atom. The similarity in the ROS levels invoked by the complexes **8** and **14** in Jurkat cells despite their very different bidentate ligands suggests that specific non-covalent interactions involving the [9]aneS_3 coligand and/or kinetic factors may play an important role in the mode of action of these rhodium(III) thiaether complexes. Due to the restricted ability of its additional thiaether S atoms to neutralize the high positive charge of the central rhodium(III) atoms through σ donation (Brandt and Sheldrick 1996), a significantly slower chloride substitution rate will be expected for **14** in comparison to both the κ^2N(imino) complex **8** and, in particular, the inactive piperazine complex **13** with its more effective amino N σ donor atoms. The slower decrease in MCF-7 cell adhesion and respiration caused by **14** versus **8** (Figs. 9, 10) may, therefore, reflect its slower reaction rate with possible cellular target molecules.

Materials and methods

Chemicals

$RhCl_3 \cdot 3H_2O$ was purchased from ABCR, 1,4,7-trithiacyclononane, 9,10-diaminophenanthrene, sodium dimethyldithiocarbamate, 2-phenylpyridine and CT DNA from Sigma–Aldrich, 4,4′-dicarboxy-2,2′-bipyridine from TCI, 2,3-diaminonaphthalene from Acros Organics, 1,2-phenylenediamine from Merck and crystal violet from Roth. Concentrations of CT DNA were determined spectrophotometrically using the molar extinction coefficient $\varepsilon_{260} = 13{,}200\ M^{-1}\ cm^{-1}$ (Marmur 1961). Solvents for synthesis were analytical reagents grade (JT Baker) and were dried and distilled before use. Deuterated solvents for ^1H NMR measurements were obtained from Deutero GmbH.

Instrumentation

UV/Vis spectra were recorded on an Analytik Jena SPECORD 200, IR spectra on a Nicolet Impact 4000 spectrometer. A Jasco J-715 instrument was used to measure CD spectra for complex/CT DNA mixtures. Liquid secondary ion mas spectrometry data (LSIMS) were registered on a Fisons VG Autospec employing a cesium ion gun (17 kV), with 3-nitrobenzyl alcohol as the liquid matrix. A Bruker DRX 400 spectrometer was used for the ^1H NMR spectroscopic characterization of the new compounds, with chemical shifts reported as δ values relative to the residual signal of the deuterated solvent. The splitting of proton resonances was defined as s = singlet, d = soublet, m = multiplet. Elemental analyses were performed on a Vario EL of Elementar Analysensysteme GmbH. Compounds **7**–14 were prepared in accordance with literature procedures (Bieda et al. 2009a, 2010).

[RhCl(bpy-4,4′-$(COOH)_2$)([9]aneS_3)]$Cl_2 \cdot H_2O$ 1

92.7 mg (0.38 mmol) 2,2-bpy-4,4′-$(COOH)_2$ were suspended in 20 ml ethanol and 100.2 mg (0.38 mmol) $RhCl_3 \cdot 3H_2O$, dissolved in 20 ml ethanol, were added and the colourless suspension was refluxed at 100°C for 2 h. Addition of 68.2 mg (0.38 mmol) [9]aneS_3 to the resulting orange solution followed by refluxing at 100°C for a further 4 h led to formation of a yellow suspension. After filtration, the

solution was reduced in volume to 5 ml and addition of diethylether led to precipitation of the product which was washed with EtOH and dried in vacuo. Yield: 198.9 mg (80%), $C_{18}H_{20}N_2O_4Cl_3S_3Rh{\cdot}H_2O$ (651.85 g/mol) calcd. (%): N 4.30 C 33.17 H 3.4 S 14.76, found (%): N 4.1 C33.1 H 3.4 S 14.5; LSIMS m/z (%) = 561.9 (87) $[M\text{-}Cl\text{-}HCl]^+$, 526.9 (28) $[M\text{-}Cl\text{-}2HCl]^+$, 497.9 (43) $[M\text{-}Cl\text{-}HCl\text{-}CH_2CH_2]^+$, 465.9 (15) $[M\text{-}Cl\text{-}HCl\text{-}SCH_2CH_2]^+$, 437.9 (23) $[M\text{-}Cl\text{-}HCl\text{-}S(CH_2CH_2)_2]^+$; ^{1}H-NMR (MeOH-d4, 400 MHz, 25°C): δ = 3.05–3.89 (m, 12 H, CH_2 [9]aneS_3), 8.26 (d, 2H, H3/H8), 9.25 (dd, 2H, H2/H9) 9.37 (s, 2H, H5/H6) ppm.

[RhCl(phi)([9]aneS_3)]$Cl_2{\cdot}1.5H_2O$ 2

Preparation as for [RhCl(bpy)([9]aneS_3)]Cl_2 [28] with 77.1 mg of phi (0.38 mmol), suspended in 10 ml CH_2Cl_2/EtOH/CH_3Cl (4/2/1). Yield: 170 mg (72%); $C_{20}H_{22}Cl_3N_2S_3Rh_1{\cdot}1.5H_2O$ (622.89 g/mol) calcd. (%): N 4.5 C 38.56 H 4.05 S 15.4, found (%) N 3.7 C 38.8 H 4.0 S 14.9; LSIMS m/z (%) = 595.3 (14) $[M\text{-}H]^+$, 524.3 (15) $[M\text{-}Cl\text{-}HCl]^+$, 443.3 (100) $[M\text{-}S_3(CH_2CH_2)_2]^+$, 414.2 (56) $[M\text{-}[9]aneS_3\text{-}H]^+$, ^{1}H-NMR ($CD_2Cl_2$, 400 MHz, 25°C): δ = 2.90–4.01 (m, 12H, CH_2 [9]aneS_3), 7.49 (t, 2H, H3/H8), 7.74 (t, 2H, H4/H7), 8.05–8.20 (2d, 4H, H2/H9, H5/H6) ppm.

[RhCl(naphdiamine)([9]aneS_3)]$Cl_2{\cdot}H_2O$ 3

Preparation as for [RhCl(dpq)([9]aneS_3)]Cl_2 [28] with 60.1 mg 2,3-diaminonaphthalene (0.38 mmol), dissolved in 10 ml CH_2Cl_2. Yield: 86.4 mg (40%), $C_{16}H_{22}N_2Cl_3Rh_1S_3{\cdot}H_2O$ (565.82 g/mol) calcd. (%): N 4.95 C 33.96 H 4.28 S 17.0, found (%): N 4.6 C 33.9 H 4.6 S 17.1; LSIMS m/z (%) = 511.0 (34) $[M\text{-}Cl]^+$, 475 (78) $[M\text{-}Cl\text{-}HCl]^+$, 439.1 (32) $[M\text{-}Cl\text{-}2HCl]^+$, 489.1 (100) $[M\text{-}SCH_2CH_2{+}2H]^+$, ^{1}H-NMR (DMSO-$d_6$, 400 MHz, 25°C): δ = 3.70–3.90 (m, 12H, CH_2 [9]aneS_3), 7.50–7.60 (m, 2H), 7.90–8.05 (m, 4H) ppm.

[RhCl(dab)([9]aneS_3)]$Cl_2{\cdot}2H_2O$ 4

Preparation as for [RhCl(bpy)([9]aneS_3)]Cl_2 [28] with 41.6 mg 2-phenylenediamine (dab) (0.38 mmol), dissolved in 10 ml MeOH/CH_2Cl_2. Yield: 42.5 mg (21%), $C_{12}H_{20}Cl_3N_2S_3Rh{\cdot}2H_2O$ (533.79 g/mol) calcd. (%): N 5.27 C 27.0 H 4.53 S 18.02, found (%): N 5.25 C 27.3 H 4.0 S 18.5; LSIMS m/z (%) = 461.0 (15) $[M\text{-}Cl]^+$, 425.0 (40) $[M\text{-}Cl\text{-}HCl]^+$, 389.1 (93) $[M\text{-}Cl\text{-}2HCl]^+$, 281.1 (23) $[M\text{-}Cl\text{-}2HCl\text{-}dab]^+$, 329.1 (17) $[M\text{-}Cl\text{-}2HCl\text{-}(CH_2CH_2S)]^+$, ^{1}H-NMR (DMSO-$d_6$, 400 MHz, 25°C): δ = 3.13–3.85 (m, 12H, CH_2 [9]aneS_3), 7.17–7.75 (m, 4H, dab) ppm.

[RhCl(dmdtc)([9]aneS_3)]$(CF_3SO_3){\cdot}2H_2O$ 5

100 mg (0.18 mmol) of $[RhCl_2(MeCN)([9]aneS_3)](CF_3SO_3){\cdot}1.5\ H_2O$ [30] were dissolved in 15 ml MeOH and 33.2 mg of $Na[S_2CNMe_2]$ (0.18 mmol), dissolved in 2 ml MeOH, were added. The reaction mixture was refluxed for 3 h. Following filtration of the yellow precipitate and volume reduction of the remaining orange solution to 5 ml, addition of diethyl ether led to precipitation of the product, which was washed with MeOH and dried in vacuo. Yield: 66.7 mg (61%), $C_{10}H_{18}ClNO_3S_6F_3Rh{\cdot}2H_2O$ (622.85 g/mol) calcd. (%): N 2.24 C 19.25 H 3.55 S 30.83, found (%): N 1.8 C 18.8 H 3.1 S 30.4; LSIMS m/z (%) = 437.8 (100) $[M\text{-}OTf]^+$, 402.8 (44) $[M\text{-}HOTf\text{-}Cl]^+$ 374.8 (13) $[M\text{-}HOTf\text{-}Cl\text{-}CH_2CH_2]^+$ 345.8 (4) $[M\text{-}HOTf\text{-}Cl\text{-}(CH_2CH_2)_2]^+$, 314.8 (13) $[M\text{-}HOTf\text{-}Cl\text{–}S(CH_2CH_2)_2]^+$, ^{1}H-NMR ($CD_3CN$, 400 MHz, 25°C): δ = 3.19 (s, 6H, CH_3 carbamate), 3.16–3.22 (m, 8H, CH_2 [9]aneS_3), 3.34–3.46 (m, 4H, CH_2 [9]aneS_3) ppm.

[RhCl(phenylpy)([9]aneS_3)]$Cl{\cdot}3H_2O$ 6

500 µl 30% NaOMe (0.38 mmol) were added to 54.3 µl 2-phenylpyridine (0.38 mmol) and were stirred at 37°C for 24 h. 100 mg of $RhCl_3{\cdot}3H_2O$ (0.38 mmol) dissolved in 30 ml MeOH/CH_2Cl_2 (1/1) was added and the reaction mixture was heated for 2 h in boiling MeOH/CH_2Cl_2. After addition of 68.4 mg of [9]aneS_3 (0.38 mmol), the resulting suspension was refluxed for a further 5 h. Following filtration of the yellow precipitate ([$RhCl_3$([9]aneS_3)]) and volume reduction of the remaining solution to 5 ml, addition of diethyl ether led to precipitation of the product, which was washed with H_2O and dried in vacuo. Yield: 25.2 mg (72%), $C_{17}H_{20}NCl_2S_3Rh_1{\cdot}3H_2O$ (562.4 g/mol) calcd. (%): N 2.49 C 36.31 H 4.66 S 17.1, found (%): N 2.45 C 36.51 H 4.61 S 16.45; LSIMS m/z (%) = 471.9 (100) $[M\text{-}Cl]^+$,

437.1 (6) $[M\text{-}Cl\text{-}HCl]^+$, ^{1}H-NMR ($D_2O$ + NaCl, 400 MHz, 25°C): δ = 3.4–3.75 (m, 12H, CH_2 [9]aneS_3), 7.28–7.53 (m, 3H, H3/H7/H8), 7.77 (d, 1H, H6), 7.95 (dd, 1H, H5), 8.12 (t, 1H, H4), 8.27 (d, 1H, H9), 8.74 (d, 1H, H2) ppm.

Biological investigations

Cell cultures

MCF-7 breast adenocarcinoma and HT-29 colon carcinoma cells were maintained in DMEM High Glucose (PAA) supplemented with 50 mg l^{-1} gentamycin and 10% (v/v) fetal calf serum (FCS) at 37°C/5% CO_2 and passaged once a week according to standard procedures. For HEK-293 cells, Dulbecco's modified eagle medium (Invitrogen) supplemented with 10% fetal bovine serum and 100 units/ml penicillin and streptomycin was employed at 37°C/5% CO_2. The cells were split and aliquots were seeded in 35 mm culture dishes three times a week. Burkitt-like lymphoma BJAB cells were maintained at 37°C in RPMI 1640 (GIBCO, Invitrogen) supplemented with 10% heat-inactivated FCS, penicillin (100,000 U l^{-1}), streptomycin (0.1 g l^{-1}) and L-glutamine (0.56 g l^{-1}). The cells were subcultured every 3–4 days by dilution of the cells to a concentration of 1×10^5 cells ml^{-1}. Twenty-four hours before the assay setup, cells were cultured at a concentration of 3×10^5 cells ml^{-1} to ascertain standardized growth conditions. For the apoptosis assays, the cells were then diluted to a concentration of 1×10^5 cells ml^{-1} immediately before addition of the complexes.

Antiproliferative activity measurements

The antiproliferative effects of the compounds were determined by an established procedure for the MCF-7 and HT-29 cells (Ott et al. 2005). An adaption of the procedure was employed for the HEK-293 cells (Bieda et al. 2010). Initial determination of a growth curve led to the HEK-293 specific parameters of cell concentration and incubation periods. Cells were suspended in cell culture medium (MCF-7: 10000 cells ml^{-1}; HT-29: 2,850 cells ml^{-1}; HEK-293: 2,000 cells ml^{-1}) and 100 µl aliquots thereof were plated in 96 well-plates and incubated at 37°C/5% CO_2 for 72 h (MCF-7), or 48 h (HT-29 or HEK-293). In analogy to the procedure for MCF-7 and HT-29 cells, one plate was subsequently used for the determination of the initial HEK-293 cell biomass. Following removal of the medium, the HEK-293 cells were fixed by a 20–30 min incubation with 100 µl glutardialdehyde solution (1 ml glutardialdehyde in 25 ml PBS, pH 7.3). The solution was removed, 180 µl PBS were added and the plate stored at 4°C until further treatment. Stock solutions of the compounds **1–6** in DMF were freshly prepared and diluted with cell culture medium to the desired concentrations (final DMF concentration: 0.1% v/v). The medium in the plates was replaced with medium containing the compounds at graded concentrations (six replicates). After further incubation for 96 h (MCF-7), 72 h (HT-29) or 96 h (HEK-293), the medium was removed and the plates treated with glutardialdehyde and PBS as described above. The cell biomass was determined for HEK-293 and the other cells by crystal violet staining using the following procedure. Firstly, the PBS was removed before addition of 100 µl of 0.02 M crystal violet solution and the plates were incubated for 30 min. The crystal violet solution was subsequently removed, and the fixed cells were then washed twice with water and exposed to water for 15 min. The water was removed and the crystal violet extracted from the adherent cell biomass by shaking for 3 h on a softly rocking rotary shaker with 180 µl of 70% ethanol. The absorption was then determined at 590 nm using a Fusion α multiwell-plate reader (Perkin–Elmer) for HEK-293 cells, or a Victor X4 2030 Multilabel Reader for MCF-7 and HT-29 cells. The mean absorption of the initial biomass plate was subtracted from the mean absorption of each experiment and control. IC_{50} values were determined as those concentrations causing 50% inhibition of cell proliferation. Results were calculated from 2 to 3 independent experiments.

Annexin-V propidium iodide binding assay for Jurkat and K562 cells

Jurkat cells were purchased from German Collection of Microorganisms and Cell Culture (DSMZ, Braunschweig, No AA 282, LOT 7). The cells were maintained in RPMI 1640 (PAA) medium supplemented with 10% fetal calf serum (FCS, PAA), 37°C,

5% CO_2 and maximum humidity. Jurkat/K562 cells were cultivated in standard conditions.

After harvesting Jurkat cells/K562 cells and an incubation period of either 24 or 48 h, the cells were washed in cold phosphate-buffered saline (PBS). **N**egative controls were prepared by incubating cells in the absence of inducing agent. After resuspension at a concentration of 1×10^6 cells/ml in an annexin binding buffer (10 mM HEPES, 140 mM NaCl, and 2.5 mM $CaCl_2$, pH 7.4.), 100 µl of this suspension were prepared to provide a sufficient volume per assay. 5 µl of the annexin V conjugate (in 25 mM HEPES, 140 mM NaCl, 1 mM EDTA, pH 7.4, plus 0.1% bovine serum albumin (BSA); obtained from Invitrogen) were added together with the dead-cell indicator such as propidium iodide (SYTOX® Green dye) to each 100 µl of cell suspension. After an incubation period of 15 min at room temperature, the cells were analyzed by flow cytometry using a FACS®Calibur (Becton–Dickinson) and the CellQuest Pro (BD) analysis software.

PARP cleavage

Jurkat cells were incubated with different amounts of selected compounds for 24 h. Cell lysing and analyzing were performed in a 10% SDS–PAGE. Proteins were transferred on Immobilon-P Transfer membranes (Milipore) and the immune blotting was performed with anti-PARP rabbits polyclonal antibodies. For the signal detection a western blot lightning ECL-reagent and a LAS 3000 Imaging system (Fuji) were used.

Measurement of intracellular ROS towards the Jurkat and K562 cell lines

Jurkat cells were cultivated in standard conditions during the treatment and the cells were treated with indicated concentrations of the substances for 3 and 9 h. Cells were collected at given time points, centrifuged at 0.2 g (1,500 rpm) and resuspended in FACS buffer (D-PBS, Gibco, +1% BSA, PAA). The cell suspension was incubated with DHE (dihydroethidium, SIGMA, 5 µl of 5 mM stock solution per 1 ml of cell suspension containing 10^6 cells) at room temperature in the dark for 15 min., washed once more with FACS buffer and immediately analysed using a FACS®Calibur (Becton–Dickinson) and CellQuest Pro (BD) analysis software. Excitation and emission settings were 488 nm and 564–606 nm (FL2 filter), respectively. The region of 'low'- and 'high'- ROS on histogram plot were determined according to the corresponding control samples.

Cellular metabolism

Changes in cellular metabolism and morphology were analyzed using a Bionas 2500 sensor chip system (Bionas, Rostock, Germany). The sensor chip (SC1000) enables continuous measurement of oxygen consumption using oxygen-sensitive electrodes (Wolf et al. 1998), pH changes of the medium by employing ion-sensitive field effect transistors (Lehmann et al. 2000) and the impedance between two interdigitated electrode structures (Ehret et al. 1998) to register the impedance under and across the cell layer on the chip surface. Before measurement, cells were seeded on the sensor chip in DMEM (PAA, E15-883) with penicillin/streptomycin and 10% (v/v) FCS (PAA) and incubated in a standard tissue culture incubator at 37°C/5% CO_2 and 95% humidity for 24 h until 90% confluency was reached. Sensor chips with cells were then transferred to the Bionas 2500 analyzer in which medium is continuously exchanged in 10 min cycles (3 min exchange of medium and 7 min without flow) during which the parameters were measured. The running medium used during the analysis was DMEM without carbonated buffer (PAN Cat. Nr. P03-0010) and only weakly buffered with 1 mM Hepes, reduced FCS (0.1%) and low glucose (1 g l^{-1}). For drug activity testing, the following steps were followed: (a) 5 h equilibration with running medium with 3 and 7 min stop/flow incubation intervals, (b) 38 h drug incubation with substances freshly dissolved in medium at indicated concentrations also with the same stop/flow, and (c) a 9 h step in which the cells were again fed with running medium without substances. At the end of each experiment, cells were killed by addition of 0.2% Triton X-100 to obtain a basic signal without living cells on the sensor surface with as a negative control.

Acknowledgments Financial support for this work in Bochum, Braunschweig and Heidelberg by the Deutsche Forschungsgemeinschaft (DFG) within the research group

FOR 630 "Biological function of organometallic compounds" is gratefully acknowledged. Ruth Bieda wishes to thank the Ruhr University Research School for the award of a scholarship.

References

Andree HA, Reutelingsperger CP, Hauptmann HC, Hemker HC, Hermens WT, Willems GM (1990) Binding of vascular anticoagulant-alpha (vac-alpha) to planar phospholipid-bilayers. J Biol Chem 265:4923–4928

Annen P, Schildberg S, Sheldrick WS (2000) (η^5-Pentamethylcyclopentadienyl)iridium(III) complexes of purine nucleobases and nucleotides: a comparison with (η^6-arene)ruthenium(II) and (η^5-pentamethylcyclopentadienyl)rhodium(III) species. Inorg Chim Acta 307:115–124

Bieda R, Ott I, Dobroschke M, Prokop A, Gust R, Sheldrick WS (2009a) Structure-activity relationships and DNA binding properties of apoptosis inducing cytotoxic rhodium(III) polypyridyl complexes containing the cyclic thioether [9]aneS$_3$. J Inorg Biochem 103:698–708

Bieda R, Ott I, Gust R, Sheldrick WS (2009b) Cytotoxic rhodium(III) polypyridyl complexes containing the tris(pyrazolyl)methane coligand: synthesis, DNA binding properties and structure-activity relationships. Eur J Inorg Chem 3821–3831

Bieda R, Dobroschke M, Triller A, Ott I, Spehr M, Gust R, Prokop A, Sheldrick WS (2010) Cell-selective, apoptosis-inducing rhodium(III) crown thiaether complexes. ChemMedChem 5:1123–1133

Brabec V, Kleinwächter V, Butour J-L, Johnson NP (1990) Biophysical studies of the modification of DNA by antitumor platinum coordination complexes. Biophys Chem 25:129–141

Brandt K, Sheldrick WS (1996) Synthesis, structure and reactivity of the thioether half-sandwich rhodium complex [RhCl(MeCN)$_2$([9]aneS$_3$)][CF$_3$SO$_3$]$_2$. J Chem Soc Dalton Trans 1237–1243

Clarke M (2002) Ruthenium metallopharmaceuticals. Coord Chem Rev 232:69–93

Dobroschke M, Geldmacher Y, Ott I, Harlos M, Kater L, Wagner L, Gust R, Sheldrick WS (2009) Cytotoxic rhodium(III) and iridium(III) polypyridyl complexes: structure-activity relationships, antileukemic activity, and apoptosis induction. ChemMedChem 4:177–187

Ehret R, Baumann W, Brischwein M, Schwinde A, Wolf B (1998) Online control of cellular adhesion with impedance measurements using interdigitated electrode structures. Med Biol Eng Comput 36:365–370

Eriksson M, Norden B (2001) Linear and circular dichroism of drug-nucleic acid complexes. Methods Enzymol 340: 60–98

Erkkila KE, Odom DT, Barton JK (1999) Recognition and reaction of metallointercalators with DNA. Chem Rev 99:2777–2795

Frodl A, Herebian D, Sheldrick WS (2002) Coligand tuning of the DNA binding properties of bioorganometallic (arene)ruthenium(II) complexes of the type [(arene)Ru(amino acid)(dppz)]$^{n+}$ (dppz = dipyrido[3,2-*a*:2′,3′-*c*]phenazine), n = 1-3. J Chem Soc Dalton Trans, 3664–3673

Harlos M, Ott I, Gust R, Alborzinia H, Wölfl S, Kromm A, Sheldrick WS (2008) Synthesis, biological activity, and structure-activity relationships for potent cytotoxic rhodium(III) polypyridyl complexes. J Med Chem 51: 3924–3933

Hartinger CG, Zorbas-Seifried S, Jakupec MA, Kynast B, Zorbas H, Keppler BK (2006) From bench to bedside—preclinical and early clinical development of the anticancer agent imidazolium trans-[tetrachlorobis(1H-indazole)ruthenium(III)] (KP1019 or FFC14A). J Inorg Biochem 100:891–904

Herebian D, Sheldrick WS (2002) Synthesis and DNA binding properties of bioorganometallic (pentamethylcyclopentadienyl)iridium(III) complexes of the type [(C$_5$Me$_5$)Ir(-Aa)(dppz)]$^{n+}$ (dppz = dipyrido[3,2-*a*:2′,3′-*c*]-phenazine, n = 1-3), with S-coordinated amino acids (Aa) or peptides. J Chem Soc Dalton Trans 966–974

Jakupec MA, Galanski M, Arion VB, Hartinger CG, Keppler BK (2008) Antitumor metal complexes: more than theme and variations. Dalton Trans, 183–194

Kapitza S, Jakupec MA, Uhl M, Keppler BK, Marian B (2005) The heterocyclic ruthenium(III) complex KP1019 (FFC14A) causes DNA damage and oxidative stress in colorectal tumor cells. Cancer Letts 226:115–121

Koopman G, Reutelingsperger CPM, Kuijten GAM, Keehnen RMJ, Pals ST, van Oers MHJ (1994) Annexin-V for flow cytometric detection of phosphatidylserine expression on B-cells undergoing apoptosis. Blood 84:1415–1420

Lecoeur H (2002) Nuclear apoptosis detection by flow cytometry: influence of endogenous endonucleases. Exp Cell Res 277:1–14

Lehmann M, Baumann W, Brischwein M, Ehret R, Kraus M, Schwinde A, Bitzehofer M, Freud I, Wolf B (2000) Noninvasive measurement of cell membrane associated proton gradients by ion-sensitive field effect transistor arrays for microphysiological and bioelectronical applications. Biosens Bioelectron 15:117–124

Levina A, Mitra A, Lay PA (2009) Recent developments in ruthenium anticancer drugs. Metallomics 1:458–470

Madureira J, Santos TM, Goodfellow BJ, Lucena M, Pedrossa de Jesus J, Santana-Marques MG, Drew MGB, Felix Y (2000) Structural characterisation of new Ru-II[9]aneS(3) polypyridyl complexes. J Chem Soc Dalton Trans 4422–4431

Marmur J (1961) Procedure for isolation of deoxyribonucleic acid from micro-organisms. J Mol Biol 3:208–218

Medvetz DA, Stakleff KD, Schreiber T, Custer PD, Hindi K, Panzner MJ, Blanco D, Taschner MJ, Tessier CA, Youngs WJ (2007) Ovarian cancer activity of cyclic amines and thiaether metal complexes. J Med Chem 50:1703–1706

Menon EL, Perea R, Navarro M, Kuhn RJ, Morrison H (2004) Phototoxicity against tumor cells and sindbis virus by an octahedral rhodium bispyridyl complex and evidence for the genome as a target in viral photoinactivation. Inorg Chem 43:5373–5381

Metcalfe C, Thomas JA (2003) Kinetically inert transition metal complexes that reversibly bind to DNA. Chem Soc Rev 32:215–224

Morbidelli L, Donnini S, Filippi S, Messori L, Piccioli F, Orioli P, Sava G, Ziche M (2003) Antiangiogenic properties of

selected ruthenium(III) complexes that are nitric oxide scavengers. Br J Cancer 88:1481–1491

Nicholson DW, Ali A, Thornberry NA, Vallancourt JP, Ding CK, Gallant M (1995) Identification and inhibition of the ice/ced-3 protease necessary for mammalian apoptosis. Nature 376:37–43

Ott I, Gust R (2007) Non platinum metal complexes as anticancer drugs. Arch Pharm Chem Life Sci 340:117–126

Ott I, Schmidt K, Kircher B, Schuhmacher P, Wiglenda T, Gust R (2005) Antitumor-active cobalt-alkyne complexes derived from acetylsalicyclic acid. Studies of the mode of drug action. J Med Chem 48:622–629

Pruchnik FP, Jakimowicz P, Ciunik Z, Zakrzewska-Czerwinska J, Opolski A, Wietrzyk J, Wojdat E (2002) Rhodium(III) complexes with polypyridyls and pyrazole and their antitumor activity. Inorg Chim Acta 334:59–66

Rademaker-Lakhai JM, Van den Bongard D, Pluim D, Beijnen JH, Schellens JHM (2004) A phase I and pharmocological study with imidazolium-trans-DMSO-imidazole-tetrachlororuthenate—a novel ruthenium anticancer agent. Clin Cancer Res 10:3717–3727

Riccardi C, Nicoletti I (2006) Analysis of apoptosis by propidium iodide staining and flow cytometry. Nat Protoc 1:1458–1461

Rosenberg B, VanCamp L, Trosko JE, Mansour VH (1969) Platinum compounds—a new class of antitumor agents. Nature 222:385

Sandstrom PA, Mannie MD, Buttke TM (1994) Inhibition of activation-induced death in T-cell hybridomas by thiol antioxidants—oxidative stress as a mediator of apoptosis. J Leukoc Biol 55:221–226

Schäfer S, Ott I, Gust R, Sheldrick WS (2007) Influence of the polypyridyl (pp) ligand size on the DNA binding properties, cytotoxicity and cellular uptake of organoruthenium(II) complexes of the type $[(C_6Me_6)Ru(L)(pp)]^{n+}$ [L = Cl, $n = 1$; L = $(NH_2)_2CS$, $n = 2$]. Eur J Inorg Chem 3034–3046

Scharwitz MA, Ott I, Geldmacher Y, Gust R, Sheldrick WS (2008) Cytotoxic half-sandwich rhodium(III) complexes: polypyridyl ligand influence on their DNA binding properties and cellular uptake. J Organomet Chem 693: 2299–2309

Sheldrick WS, Hagen-Eckhard HS, Heeb S (1993) Preparation and structural characterization of tetranuclear (η^6-benzene)ruthenium(II) complexes with bridging N-donor atoms. Inorg Chim Acta 206:15–21

Shields TP, Barton JK (1995) Sequence-selective DNA recognition and photocleavage—a comparison of enantiomers of Rh(en)2Phi(3+). Biochemistry 34:15037–15048

Simon H-U, Hai-Yehia A, Levi-Schäfer F (2000) Role of reactive oxygen species (ROS) in apoptosis induction. Apoptosis 5:418–425

Sitlani A, Long EC, Pyle AM, Barton JK (1992) DNA photocleavage by phenanthrenequinone diimine complexes of rhodium(III)—shape-selective recognition and reaction. J Am Chem Soc 114:2303–2312

Van Engeland M, Nieland LJW, Ramaekers FCS, Schutte B, Reutelingsperger CPM (1998) Annexin V-affinity assay: a review on an apoptosis detection system based on phosphatidylserine exposure. Cytometry 31:1–9

Wang Y, Zhang X, Zhang Q, Yang Z (2010) Oxidative damage to DNA by 1, 10-phenanthroline/L-threonine copper(II) complexes with chlorogenic acid. Biometals 23:265–273

Wolf B, Brischwein M, Baumann W, Ehret R, Kraus M (1998) Monitoring of cellular signaling and metabolism with modular server technique: the PhysioControl Microsystem (PCM). Biosens Bioelectron 13:501–509

Zeglis BM, Pierre VC, Barton JK (2007) Metallo-intercalators and metallo-insertors. Chem Commun 4565–4579